Polymer 50 (2009) 1559–1565

Contents lists available at ScienceDirect

Polymer

journal homepage: www.elsevier.com/locate/polymer

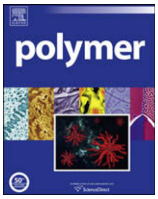

Structures and cocrystallization behavior of copolyesters based on poly(octamethylene terephthalate) and poly(octamethylene 2,6-naphthalate)

Young Gyu Jeong*, Jong Hyun Lee, Sang Cheol Lee

School of Advanced Materials and System Engineering, Kumoh National Institute of Technology, Gumi, Gyeongbuk 730-701, Republic of Korea

A R T I C L E I N F O

Article history:
Received 17 November 2008
Received in revised form
14 January 2009
Accepted 31 January 2009
Available online 6 February 2009

Keywords:
Polyesters
Cocrystallization
Melting

A B S T R A C T

We have synthesized poly(octamethylene terephthalate) (POT), poly(octamethylene 2,6-naphthalate) (PON), and poly(octamethylene terephthalate-*co*-octamethylene 2,6-naphthalate)s [P(OT-*co*-ON)s] with various comonomer composition by melt-polycondensation reaction and investigated their chain structures, crystalline structures, melting and cocrystallization behavior by using ^{1}H NMR spectroscopy, wide angle X-ray diffraction (WAXD), and differential scanning calorimetry (DSC), respectively. It was observed that P(OT-*co*-ON)s exhibit clear melting and crystallization peaks in DSC thermograms and sharp diffraction peaks in WAXD patterns throughout the copolymer composition, resulting from the cocrystallization behavior of OT and ON units in copolymers. When the melting and crystallization temperatures of P(OT-*co*-ON)s are compared as a function of the copolymer composition, there exists an eutectic point at around 23 mol% ON, where the crystal transformation from POT-type to PON-type occurs. It was confirmed from WAXD patterns of the melt-crystallized samples that the crystal transformation from POT-type to PON α-type to PON β-type occurs with the increment of the comonomer ON content in copolymers, i.e., POT-type crystals for POT and P(OT-*co*-ON) with 11 mol% ON, PON α-type crystals for P(OT-*co*-ON)s with 23–48 mol% ON, and PON β-type crystals for PON and P(OT-*co*-ON)s with 62–87 mol% ON. Both DSC and WAXD results demonstrate the isodimorphic cocrystallization of P(OT-*co*-ON)s. Based on the Wendling–Suter model for cocrystallization thermodynamics, it was found that the average defect free energy for the inclusion of OT units into PON β-type crystals is much lower than the value of the incorporation of ON units into POT-type crystals.

1. Introduction

Linear aromatic polyesters containing benzene or naphthalene rings in the backbones such as poly(alkylene terephthalate) (PAT) and poly(alkylene 2,6-naphthalate) (PAN) have gained great interest from industry and academia for last few decades, owing to their expanding applications for fibers, films, coatings, and thermoplastics [1–3]. In those polyesters, the aromatic rings give the rigidity to polymer backbones and the linear aliphatic alkylene units impart the flexibility. Therefore, by modifying the aromatic ring structures as well as the alkylene lengths, a variety of engineered polyesters with well-controlled thermal and mechanical properties could be achieved [3,4].

As members of PAT and PAN family, poly(octamethylene terephthalate) (POT) [5,6] and poly(octamethylene 2,6-naphthalate) (PON), which chemical structures are shown in Fig. 1, have high potentials as fiber and film materials but have been investigated limitedly. Thermal properties and crystal structures of poly(octamethylene terephthalate) [7] and poly(octamethylene 2,6-naphthalate) [8] have been recently reported. It was found that POT has one crystalline phase regardless of elongation and temperature [7]. From X-ray fiber diagrams and molecular modeling methods, the crystal structure of POT was identified as a triclinic with unit cell dimensions of $a = 0.456$ nm, $b = 0.560$ nm, $c = 1.870$ nm, $\alpha = 104.87°$, $\beta = 119.45°$, and $\gamma = 100.32°$. On the other hand, PON was found to be developed in two different crystalline phases of α- and β-forms, depending on the crystallization process: the α-form crystal was dominantly developed from the cold-crystallization, whereas the β-form was from the melt-crystallization [8]. The apparent melting temperatures of α- and β-form crystals were characterized to be 175 and 183 °C, respectively. In addition, the crystal structure of PON β-form, developed dominantly from the melt-crystallization, was determined to be triclinic with dimensions of $a = 0.601$ nm, $b = 1.069$ nm, $c = 2.068$ nm, $\alpha = 155.68°$, $\beta = 123.25°$, $\gamma = 52.85°$, and with the space group of $P\bar{1}$.

It has been considered that physical properties of polyesters could be easily modified by making copolyesters containing

---

* Corresponding author. Tel.: +82 54 478 7712; fax: +82 54 478 7710.
E-mail address: ygjeong@kumoh.ac.kr (Y.G. Jeong).

0032-3861/$ – see front matter © 2009 Elsevier Ltd. All rights reserved.
doi:10.1016/j.polymer.2009.01.061

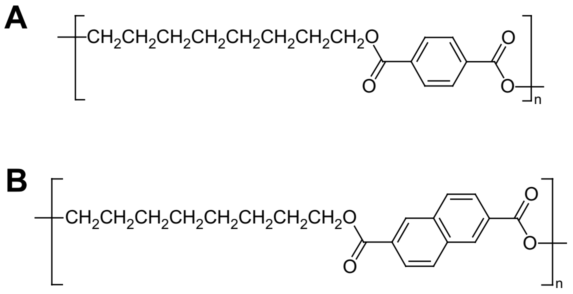

Fig. 1. Chemical structures of (A) poly(octamethylene terephthalate) (POT) and (B) poly(octamethylene 2,6-naphthalate) (PON).

different contents of benzene and/or naphthalene rings by copolymerization or reactive blending [4,9–13]. However, preparation, structures, and properties of copolyesters based on POT and PON have not been investigated. It is well-known that, in most copolyesters composed of two crystallizable *A* and *B* components, the degree of crystallinity decreases with increasing the corresponding comonomer content and as a result the copolymers often become totally amorphous even at low comonomer content. If two crystallizable components of the copolymers could coexist in their crystal lattices (i.e., cocrystallization), thermal and mechanical properties of the copolymers can be controlled without significant loss of crystalline properties [14–19]. Since the crystallographic *c*-axis length of POT is comparable with that of PON, it is highly expected that poly(octamethylene terephthalate-*co*-octamethylene 2,6-naphthalate)s [P(OT-*co*-ON)s] may exhibit a cocrystallization phenomenon. In this study, therefore, we have synthesized POT, PON, and P(OT-*co*-ON)s with various copolymer composition, characterized their chain structures using ^{1}H NMR spectroscopy and solution viscometry, and investigated their melting and crystallization behavior by using differential scanning calorimetry and wide angle X-ray diffraction method. The cocrystallization kinetics and thermodynamics of P(OT-*co*-ON)s have been also delved based on the isothermal crystallization experiments and the Wendling–Suter model, respectively.

2. Experimental

2.1. Synthesis and characterization of materials

POT, PON, and a series of P(OT-*co*-ON)s were synthesized by the two-step melt-polycondensation reactions of dimethyl terephthalate (DMT) and/or dimethyl 2,6-naphthalate (DMN) with 1,8-octanediol (OD) in the presence of titanium isopropoxide catalyst. The melt-polycondensation was carried out on a custom-designed laboratory-scale polymerisation reactor. The overall reaction scheme for synthesizing the polyesters is represented in Fig. 2. The first-step reaction was the ester-interchange reaction of DMT and/or DMN with OD at 170 °C under the flow of nitrogen gas and the second-step was the polycondensation reaction at 270 °C under high vacuum condition. When the viscosity of products in melt state reached a maximum value, the polycondensation reaction was terminated by quenching the products into cold water. The final products were dried in a vacuum oven for several days and used for characterization and analysis without further purification.

The chemical structure and quantitative copolymer composition of P(OT-*co*-ON)s were characterized with an aide of ^{1}H NMR spectroscopy. ^{1}H NMR spectra of the samples in $CDCl_3/CF_3COOD$ (5/5, v/v) solution with a small amount of tetramethylsilane (TMS) internal standard were recorded on a Bruker AMX500 FT-NMR spectrometer operating at 500 MHz. The intrinsic viscosities of the polyesters in the mixed solvents of phenol and 1,1,2,2-tetrachloroethane (5/5, v/v) were measured using an Ubbelohde viscometer at 30 °C to evaluate the relative molecular weight of the samples.

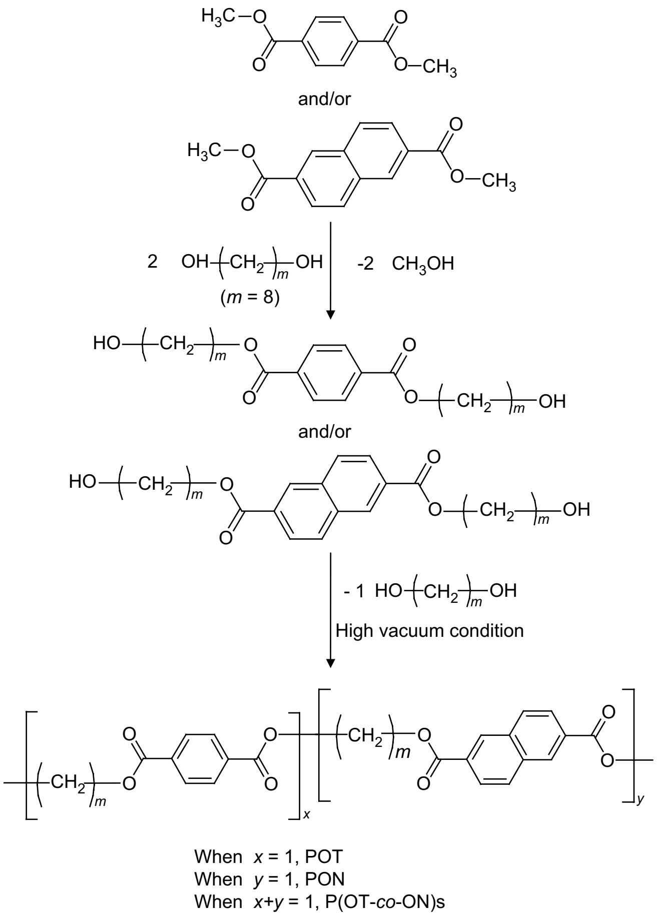

Fig. 2. Reaction scheme for synthesizing POT, PON, and a series of P(OT-*co*-ON)s with different comonomer composition.

2.2. Differential scanning calorimetry

The melting and crystallization behavior of POT, PON, and P(OT-*co*-ON)s was investigated with a differential scanning calorimeter (Perkin–Elmer DSC-7) equipped with an intercooler. DSC measurement was carried out under the flow of high purity nitrogen gas at a heating and cooling rate of 10 °C/min. For the melting and crystallization experiments, melt-quenched samples were prepared by heating the samples to the temperature 30 °C higher than their respective apparent melting temperatures, holding for 3 min, quenching into cold water, and then drying for several days under vacuum at 25 °C. The endothermic and exothermic peak temperatures of heating and cooling thermograms of the samples were taken as the apparent melting and crystallization temperatures, respectively.

Isothermal crystallization experiments were performed to study the crystallization kinetics and to determine the equilibrium melting temperatures (T_m^o) of the samples. Isothermal crystallization was carried out at various crystallization temperatures. The samples were heated to the temperature 30 °C higher than their respective apparent melting temperatures, held for 3 min to completely melt the crystals, and rapidly cooled to a predetermined crystallization temperature (T_c) at a rate of 200 °C/min. The isothermal crystallization exotherms were recorded as a function of time. After the isothermal crystallization, the samples were then heated to measure melting temperatures (T_m). The T_m^os for all the samples were determined from the linear extrapolation of T_m versus T_c plots suggested by Hoffman and Weeks [20].

2.3. Wide angle X-ray diffraction

The crystalline structures of isothermally melt-crystallized films were characterized by wide angle X-ray diffraction (WAXD). WAXD patterns were obtained using a Rigaku X-ray diffractometer with Cu-Kα radiation operated at 45 kV and 40 mA. The samples were examined in the 2θ range of 5–40° at a scanning rate of 3°/min. All the film samples of 0.2 mm thickness were prepared by compression-molding on a hot press at the temperature 30 °C higher than the apparent melting temperature of each sample, rapidly transferring to the other hot press controlled at the temperature 30 °C lower than the apparent melting temperature, and then crystallizing isothermally for hours.

3. Results and discussion

3.1. Characterization of polyesters

Copolymer composition of a series of P(OT-*co*-ON)s synthesized in this study was quantitatively determined from ^{1}H NMR spectra. Fig. 3 shows a representative ^{1}H NMR spectrum of P(OT-*co*-ON) with 48 mol% ON with peak assignment. Since protons in naphthalene ring of ON unit in copolymers are separated into two groups, *f* and *g*, due to the chemically and magnetically different environment, the copolymer composition from respective peak areas can be determined based on the following relation:

$$\frac{a+b}{2f} = \frac{d}{f} = \frac{c}{f} = \frac{e+g}{f} = \frac{2(X+Y)}{Y}, \quad X+Y = 1 \qquad (1)$$

where *a*–*f*, and *g* denote the area corresponding to the peak assigned in Fig. 3, and *X* and *Y* indicate the mole fractions of OT and ON unit in copolymers. When the copolymer composition evaluated by Eq. (1) was compared with the feed composition, it was revealed that the copolymer composition is quite similar with the feed composition, as summarized in Table 1. On the other hand, it should be noted that the structural distribution (degree of randomness) of OT and ON components in the copolymer backbones could not be evaluated from ^{1}H or ^{13}C NMR spectra. This is because, due to the existence of relatively long octamethylene units between aromatic rings, the hydrogen atoms in phenyl or naphthalene ring could not be clearly separated into three peaks corresponding to OT/OT, OT/ON (or ON/OT) and ON/ON dyads. Nonetheless, it is believed that the distribution of OT and ON units in P(OT-*co*-ON)s is statistically random because of the virtually equal reactivity of DMT and DMN with 1,8-octanediol as well as the inter- and intra-chain transesterification during the melt-polycondensation reactions.

The intrinsic viscosities of all the samples synthesized in this study were measured to be in the range of 0.79–1.08 dL/g, as listed in Table 1. This result demonstrates that all the polyesters synthesized in this study have relatively high molecular weight.

3.2. Melting, crystallization, and crystal structures

Fig. 4 represents the heating and cooling thermograms of the melt-quenched samples of POT, PON, and P(OT-*co*-ON)s. It was found that all the P(OT-*co*-ON)s exhibit a single melting and crystallization peak. This supports that P(OT-*co*-ON)s exhibit cocrystallization behavior over the entire copolymer composition owing to the

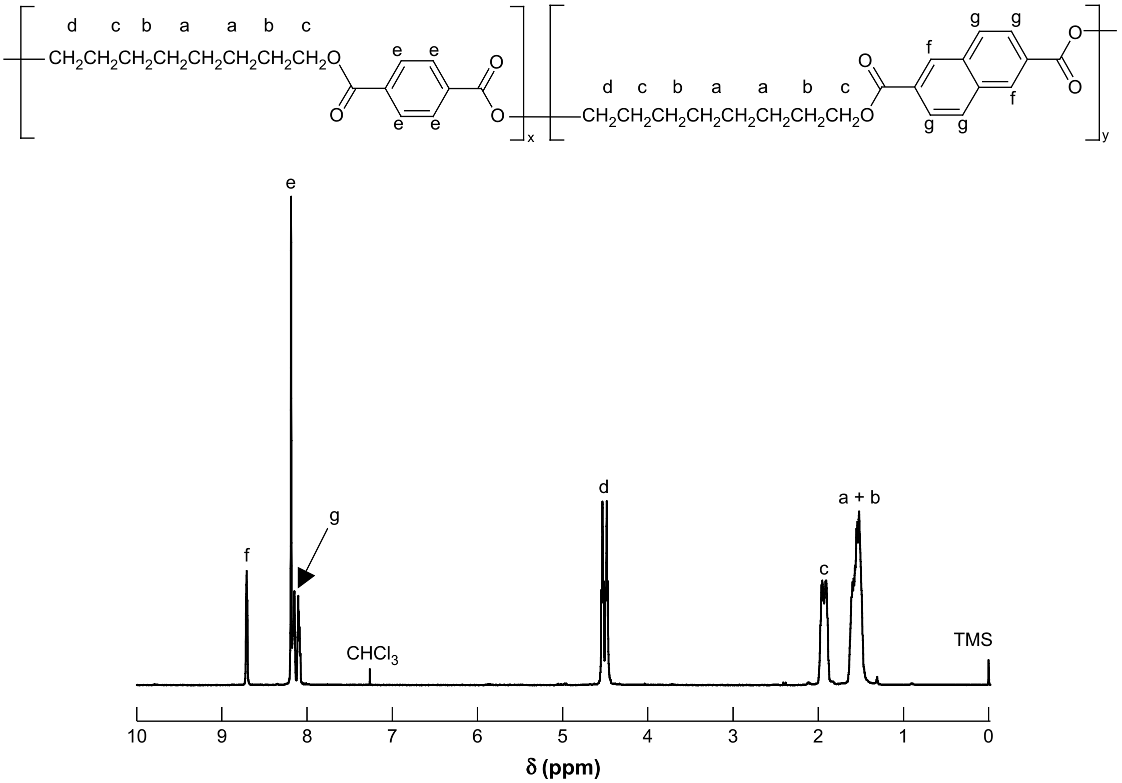

Fig. 3. A representative ^{1}H NMR spectrum of P(OT-*co*-ON) with 48 mol% ON and peak assignment.

Table 1
Composition and intrinsic viscosity of POT, PON, and P(OT-*co*-ON)s.

Sample code	Feed composition (mol% ON)	Composition by ^{1}H NMR (mol% ON)	Intrinsic viscosity (dL/g)
POT	0.0	0.0	0.99
P(OT-*co*-11 ON)	10.0	11.1	0.85
P(OT-*co*-23 ON)	25.0	23.3	0.95
P(OT-*co*-33 ON)	35.0	32.6	0.79
P(OT-*co*-48 ON)	50.0	47.6	0.92
P(OT-*co*-62 ON)	65.0	61.8	0.89
P(OT-*co*-74 ON)	75.0	74.1	0.83
P(OT-*co*-87 ON)	90.0	87.4	0.89
PON	100.0	100.0	1.08

compatibility of OT and ON units in the crystal lattices of copolymers. When the melting and crystallization temperatures of samples are compared as a function of the copolymer composition, a minimum melting and crystallization temperature corresponding to the eutectic point is observed for P(OT-*co*-ON) with around 23 mol% ON. This indicates that the crystal transformation between POT-type and PON-type happens at around 23 mol% ON. Cocrystallization is classified largely into two types, isomorphic or isodimorphic cocrystallization, depending on the existence of an eutectic point at which the crystalline structures change from one-type to the other-type [14,15,17–19,21]. Therefore, the existence of a minimum eutectic point for P(OT-*co*-ON)s in the plot of melting temperature as a function of the copolymer composition conveys the information that P(OT-*co*-ON)s exhibit an isodimorphic cocrystallization.

To investigate the influences of copolymer composition on crystalline structures of the copolyesters, we have obtained WAXD patterns for POT, PON, and P(OT-*co*-ON)s melt-crystallized isothermally at the same degree of undercooling ($\Delta T = T_m^o - T_c \sim 30$ °C), as can be seen in Fig. 5. WAXD patterns show sharp diffraction peaks originated from the crystalline regions of P(OT-*co*-ON)s over the entire copolymer composition. This result also supports cocrystallization of P(OT-*co*-ON)s, which is consistent with the DSC results. It has been reported that POT has a triclinic crystal structure [7], while PON has two different crystal structures of α- and β-forms [8], depending on the melt- and cold-crystallization process, as noted in Section 1. Close examination of WAXD patterns in Fig. 5 reveals that the crystal structures of the polyesters are divided into three major categories, i.e., POT-type crystals for POT and P(OT-*co*-11 ON), PON α-type crystals for P(OT-*co*-ON)s with 23–48 mol% ON, and PON β-type crystals for PON and P(OT-*co*-ON)s with 62–87 mol% ON. In other words, the first crystal transformation between POT and PON α-type structures occurs at the copolymer composition between 11 and 23 mol% ON, which is quite consistent with the eutectic composition observed from the DSC heating and cooling thermograms. Interestingly, the second crystal transformation from PON α- to β-type takes place at the copolymer composition between 48 and 62 mol% ON. On the other hand, it should be noted for WAXD pattern of P(OT-*co*-62 ON) in Fig. 5(f) that the diffraction peak appearing at ~19.6° is due to the existence of PON α-type crystals and other diffraction peaks are from the PON β-type crystals. It reveals that two different crystal types coexist in a copolymer, supporting the isodimorphic cocrystallization of P(OT-*co*-ON)s.

It was reported that, for PON homopolyester, PON β-type structures are dominantly developed at the melt-crystallization process, whereas the PON α-type crystals are developed at the cold-crystallization process [8]. For P(OT-*co*-ON)s with 23–48 mol% ON which exhibit diffraction patterns of PON α-type structures in Fig. 5, film samples melt-crystallized at various temperatures were prepared to find out the possibility of the crystal transformation between PON α-type and β-type. Fig. 6 displays typical WAXD patterns for P(OT-*co*-33 ON) melt-crystallized isothermally at 70–105 °C. However, P(OT-*co*-33 ON) samples exhibit only diffraction patterns of PON α-type crystals, without the crystal transformation depending on the crystallization temperatures. Hence, it is

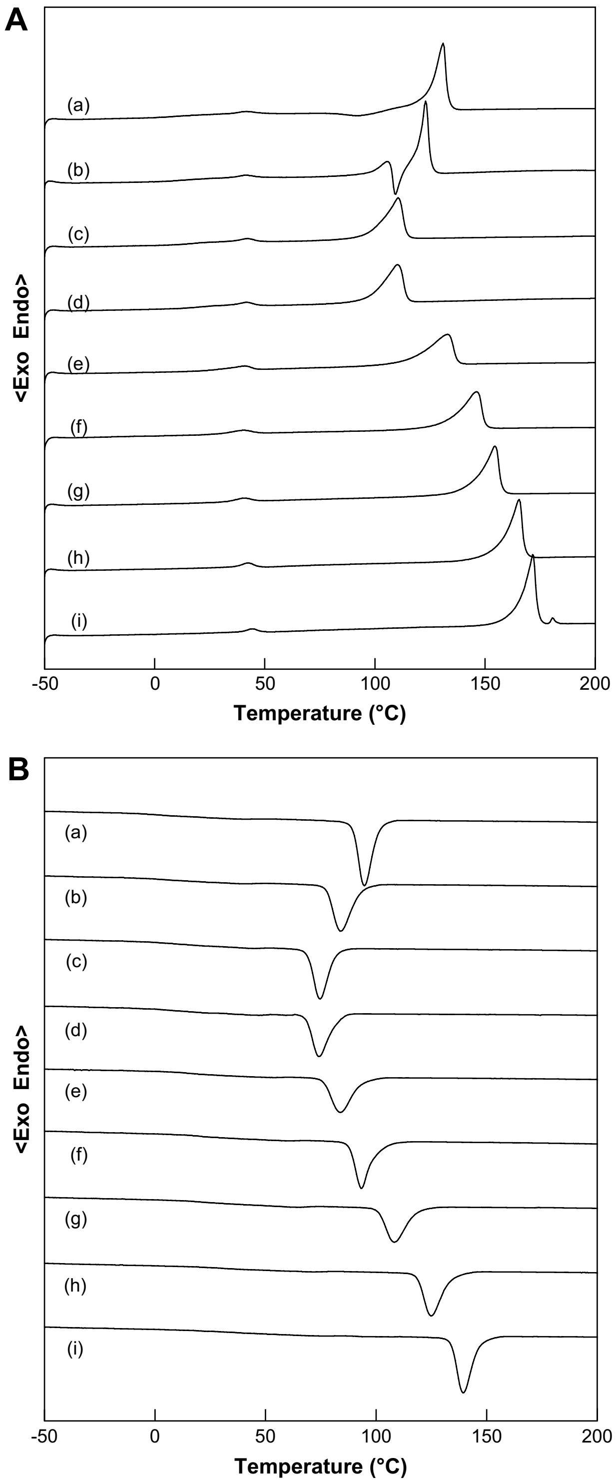

Fig. 4. Heating (A) and cooling (B) thermograms of the melt-quenched films: (a) POT; (b) P(OT-*co*-11 ON); (c) P(OT-*co*-23 ON); (d) P(OT-*co*-33 ON); (e) P(OT-*co*-48 ON); (f) P(OT-*co*-62 ON); (g) P(OT-*co*-74 ON); (h) P(OT-*co*-87 ON); (i) PON.

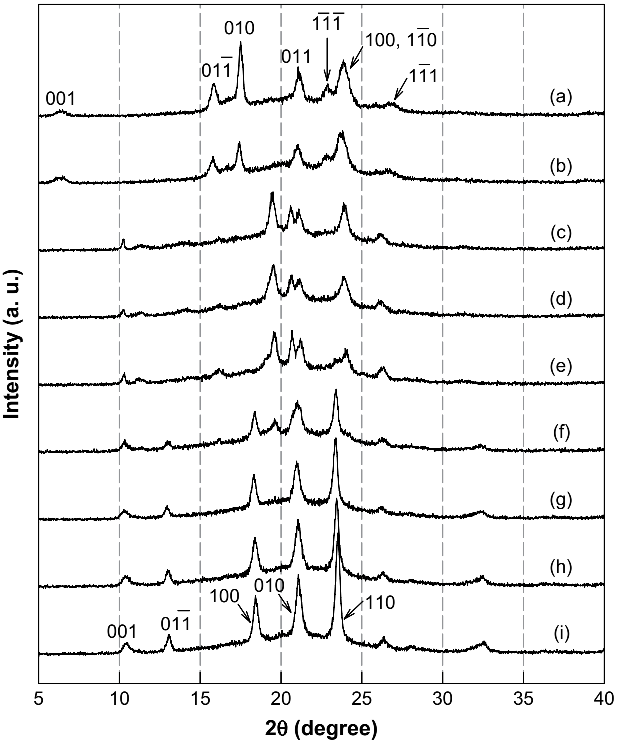

Fig. 5. WAXD patterns of film samples melt-crystallized isothermally at the same degree of undercooling ($\Delta T \sim 30\,^{\circ}C$): (a) POT; (b) P(OT-*co*-11 ON); (c) P(OT-*co*-23 ON); (d) P(OT-*co*-33 ON); (e) P(OT-*co*-48 ON); (f) P(OT-*co*-62 ON); (g) P(OT-*co*-74 ON); (h) P(OT-*co*-87 ON); (i) PON.

supposed that the PON α-type crystals developed dominantly for P(OT-*co*-ON)s with 23–48 mol% ON are induced by the existence of the comonomer OT units in the copolymer backbones, not by the temperature-induced crystal transformation.

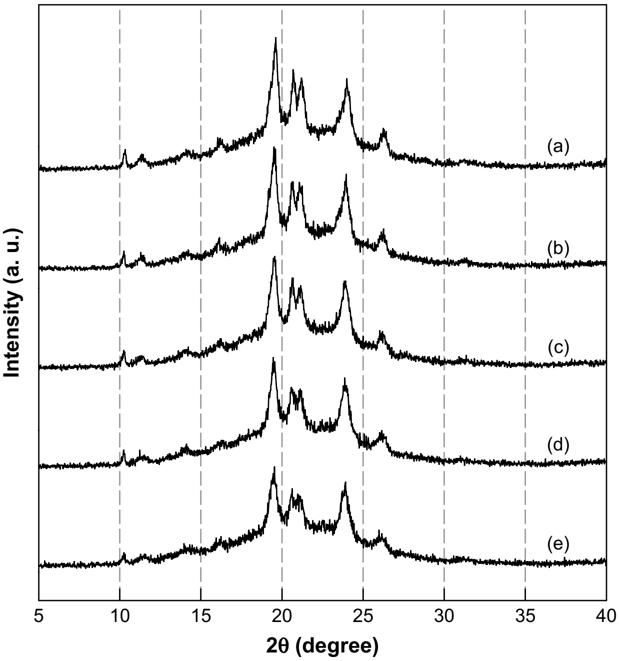

Fig. 6. WAXD patterns of P(OT-*co*-33 ON) samples melt-crystallized isothermally at various crystallization temperatures: (a) 105 °C; (b) 100 °C; (c) 90 °C; (d) 80 °C; (e) 70 °C.

The isothermal crystallization experiments were carried out for all the samples at various crystallization temperatures. Fig. 7 shows typical isothermal crystallization exotherms for POT and PON at various temperatures as a function of time. The crystallization exotherms demonstrate that the crystallization rates become slower with increasing the crystallization temperatures, as expected. To compare the relative crystallization rates of POT, PON, and P(OT-*co*-ON)s, the inverse $(t_{1/2}^{-1})$ of crystallization half time required to attain 50% of final crystallinity was evaluated as a measure of overall crystallization rate and presented as a function of degree of

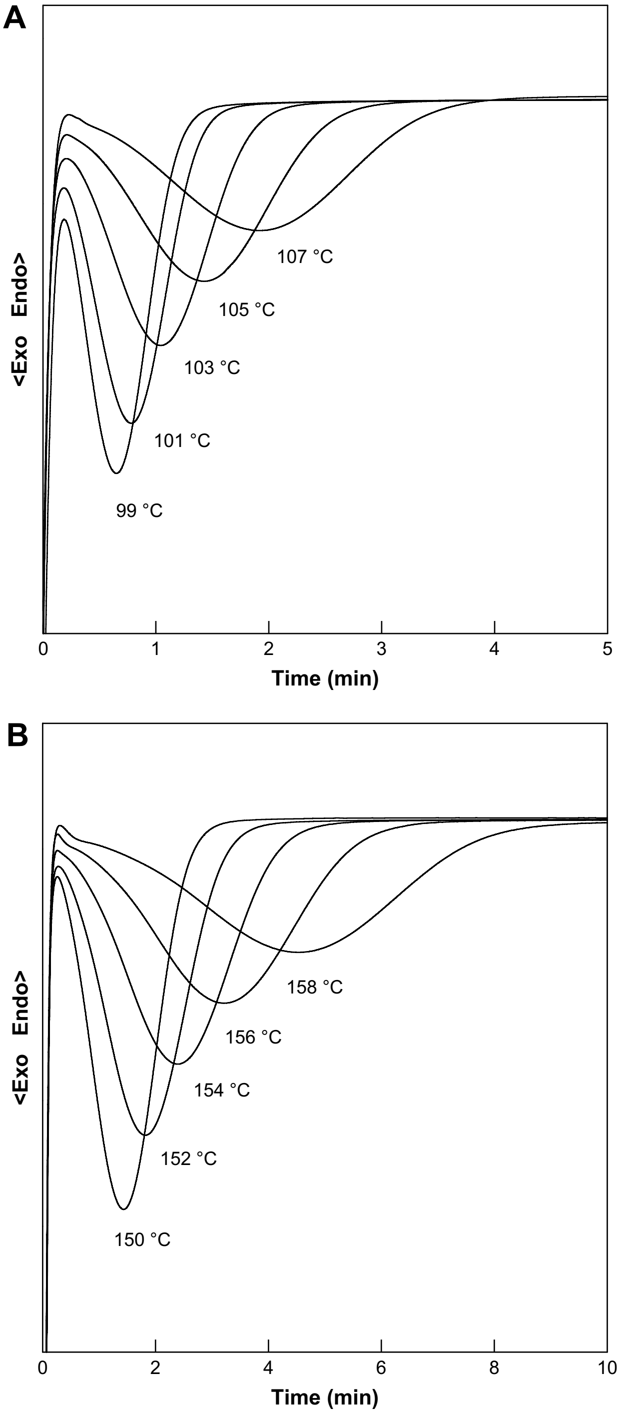

Fig. 7. Time-dependent exothermic profiles of the isothermal crystallization at various temperatures for (A) POT and (B) PON.

undercooling ($\Delta T = T_m^o - T_c$), as shown in Fig. 8. The higher value of $t_{1/2}^{-1}$ at the same degree of undercooling indicates the faster overall crystallization rate. For PON and P(OT-*co*-ON)s with 62–87 mol% ON which are developing into PON β-type crystals, the overall crystallization rates at the same degree of undercooling (for example, $\Delta T \sim 40$ °C) are decreasing as the comonomer OT content of copolymers decreases. Similarly, in cases of POT and P(OT-*co*-11 ON) which are developing into POT-type crystals, the overall crystallization rates of POT are faster than those of P(OT-*co*-11 ON) because the comonomer ON units restrict the overall crystallization of the dominant crystallizable OT units. In both cases, the overall crystallization rates of POT- or PON-based copolymers decrease with the increment of the minor comonomer content because the corresponding comonomer units retard the formation of POT-type or PON β-type cocrystals, leading to the slower crystallization rates of copolymers. On the other hand, the overall crystallization rates of P(OT-*co*-ON)s with 23 and 33 mol% ON, which are developing into PON α-type crystals, are quite comparable with POT and even faster than PON. This result is very unusual from the general concept mentioned above. From the WAXD patterns and isothermal crystallization kinetics results, it is supposed that, for P(OT-*co*-ON)s with 23 and 33 mol% ON, overall crystallization rates for developing into PON α-type crystals are much faster than those for PON β-type crystals.

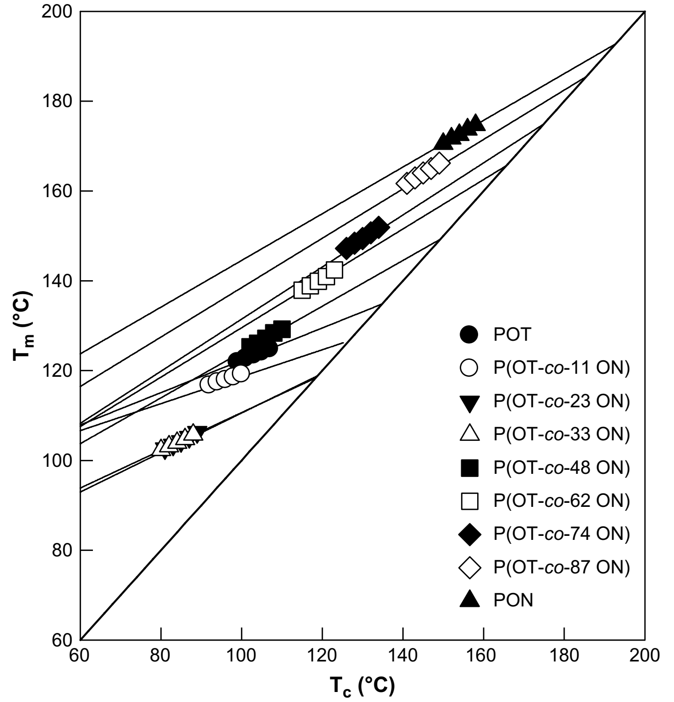

Fig. 9. Linear Hoffman–Weeks plots for evaluating equilibrium melting temperatures of POT, PON, and P(OT-*co*-ON)s.

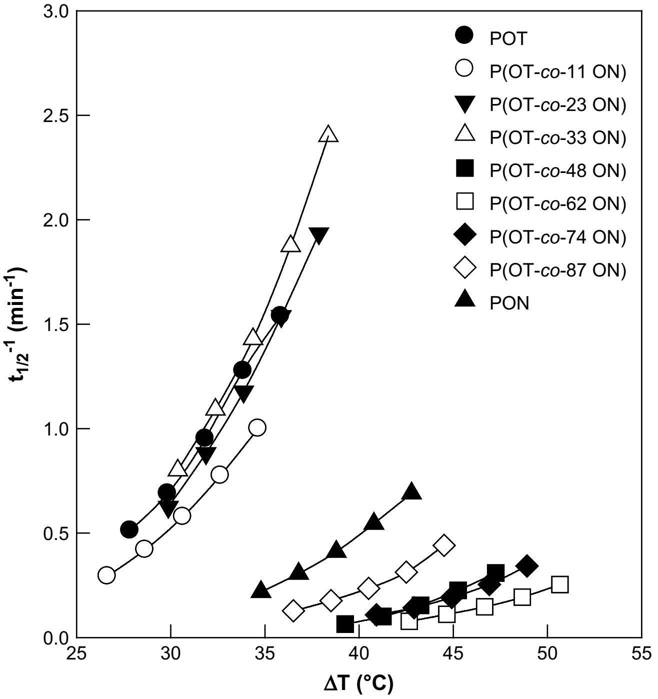

Fig. 8. The inverse ($t_{1/2}^{-1}$) of crystallization half time as a function of degree of undercooling for POT, PON, and P(OT-*co*-ON)s.

3.3. Thermodynamic analysis of cocrystallization

To understand the cocrystallization behavior of P(OT-*co*-ON)s based on the thermodynamics, we have determined equilibrium melting temperatures (T_m^o) of POT, PON, and P(OT-*co*-ON)s by using the linear extrapolation of T_m versus T_c plots suggested by Hoffman and Weeks, as shown in Fig. 9. The experimental T_m^os were plotted as a function of the comonomer ON content, as shown in Fig. 10. The T_m^os of copolymers are depressed with increasing the corresponding ON and OT commoner content of POT- and PON-based copolymers, respectively, which indicates the isodimorphic cocrystallization with an eutectic composition at around 23 mol% ON. Several theories for melting temperature depression of copolymers have been proposed and they are classified into the comonomer exclusion model [22–24] and the comonomer inclusion model [25–27]. In the present study, the melting temperature depression model proposed by Wendling and Suter [27], which unites the Sanchez–Eby model as a comonomer inclusion model with the Baur model as a comonomer exclusion model, was adopted to predict melting temperature depression of P(OT-*co*-ON)s as a function of comonomer content. The Wendling–Suter equilibrium inclusion model is as follows [27]:

$$\frac{1}{T_m^o} - \frac{1}{T_m(X_B)} = \frac{R}{\Delta H_m^o}\left[\ln\left(1 - X_B + X_B e^{-\varepsilon/RT}\right) - \left\langle\tilde{\xi}\right\rangle^{-1}\right] \qquad (2)$$

$$\left\langle\tilde{\xi}\right\rangle^{-1} = 2\left(X_B - X_B\, e^{-\varepsilon/RT}\right)\left(1 - X_B + X_B\, e^{-\varepsilon/RT}\right)$$

where T_m^o and ΔH_m^o indicate the equilibrium melting temperature and the heat of fusion of homopolymer, respectively, R the gas constant, X_B the bulk composition of comonomer B units in the copolymer, X_{CB} the concentration of comonomer B units included in the cocrystal, ε the average defect Gibbs free energy, and $\langle\tilde{\xi}\rangle$ the average length of the crystallizable copolymer sequences. The melting temperatures predicted by the equilibrium inclusion model of Eq. (2) were compared with the experimental T_m^os of POT, PON, and P(OT-*co*-ON)s by using the ε value as an adjustable parameter, as shown in Fig. 10. In such fitting works, the ΔH_m^o value of 49 kJ/mol was used for both POT and PON [28]. As a result, it was found that, when the comonomer OT units are incorporated into PON β-type crystals of P(OT-*co*-ON)s with 62–87 mol% ON, the ε values are increasing from 3.06 to 6.20 kJ/mol with the increment of the comonomer OT contents from 13 to 38 mol%. It indicates that the inclusion of the comonomer OT units into PON β-type crystals

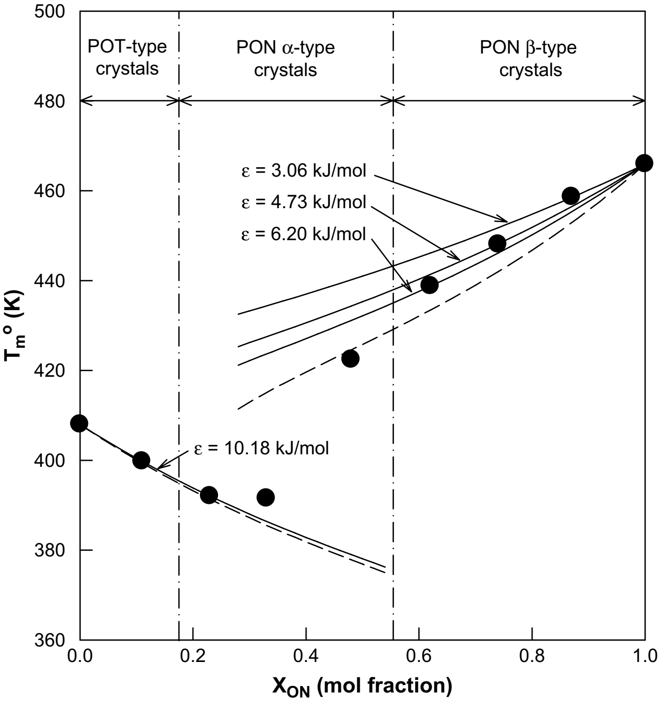

Fig. 10. Comparison of the experimental equilibrium melting temperatures of POT, PON, and P(OT-*co*-ON)s with the theoretical melting temperatures predicted by the Baur model (dashed curves) for the comonomer exclusion and the Wendling–Suter (solid lines) model for the comonomer inclusion.

becomes difficult with increasing the comonomer OT contents. In the case of P(OT-*co*-11 ON), the ε value for the inclusion of comonomer ON units into POT-type crystals is evaluated to be 10.18 kJ/mol. On the other hand, for P(OT-*co*-ON)s with 23–48 mol% ON, it is not reasonable to discuss the ε value for the inclusion of comonomer OT units in PON α-type crystals. Compared at the similar comonomer contents (for example, 11–13 mol% ON or OT), the ε value (3.06 kJ/mol) of P(OT-*co*-87 ON) in the case of the inclusion of the comonomer OT units into PON β-form crystals is much lower than the other case (10.18 kJ/mol) of P(OT-*co*-11 ON). It implies that the smaller comonomer OT units can be incorporated more easily into PON β-type crystals, compared to the opposite case. This seems to be caused by the fact that the unit cell volume (0.374 nm^3) and the crystallographic repeat length (1.870 nm) of POT is much smaller than those (0.436 nm^3 and 2.068 nm) of PON β-form, although the crystal density (1.226 g/cm^3) of POT is slightly lower than that (1.243 g/cm^3) of PON β-form.

4. Conclusions

A series of P(OT-*co*-ON)s with various comonomer contents were successfully synthesized by melt-polycondensation reaction, and characterized by solution viscometry and ^{1}H NMR spectroscopy. The inherent viscosities of all the samples were high enough to process into films. The copolymer compositions determined from ^{1}H NMR spectra were almost identical to the feed compositions. In addition, crystalline structure, melting and cocrystallization behavior of P(OT-*co*-ON)s were investigated by using wide angle X-ray diffraction (WAXD) and differential scanning calorimetry (DSC). It was observed that P(OT-*co*-ON)s exhibit clear melting and crystallization peaks in DSC thermograms and sharp diffraction peaks in WAXD patterns for all the copolymer composition as the result of the cocrystallization of OT and ON units of copolymers. When the melting and crystallization temperatures of P(OT-*co*-ON)s are compared as a function of the copolymer composition, there exists an eutectic point around 23 mol% ON, where the transformation from POT-type crystal to PON-type crystal take places. It was confirmed from WAXD patterns that the crystal transformation from POT to PON α-type to PON β-type occurs with the increment of the ON content: POT-type crystals for POT and P(OT-*co*-11 ON), PON α-type crystals for P(OT-*co*-ON)s with 23–48 mol% ON, and PON β-type crystals for PON and P(OT-*co*-ON)s with 62–87 mol% ON. Both DSC and WAXD results support that P(OT-*co*-ON)s show an isodimorphic cocrystallization. By comparing the defect free energies evaluated from the melting temperature depression model proposed by Wendling and Suter, it was found that the smaller comonomer OT units are more easily incorporated into PON β-type crystals, compared with the case of inclusion of comonomer ON units into POT-type crystals. This result is supposed to stem from the fact that the unit cell volume and the crystallographic repeat length of POT crystal are much smaller than the corresponding values of PON β-form crystal.

Acknowledgements

This paper was supported by Research Fund, Kumoh National Institute of Technology.

References

[1] Duling IN and Chester W. United States; 1969.
[2] Goodman I, Davis GW, Talbot JR, Jadhav JY, Kantor SW. Polyesters. In: Mark HF, Bikales NM, Overberger CG, Menges G, editors. Encyclopedia of polymer science and engineering, vol. 12. New York: Wiley Interscience; 1988.
[3] Schneider HA. J Appl Polym Sci 2003;88:1590–9.
[4] Sun Y-M, Shieh J-Y, Wang C-S. Eur Polym J 1997;33(3):317–23.
[5] Varma DS, Agarwal R, Varma IK. Polym Mater Sci Eng Proc ACS Dev Polym Mater 1985;53:689–92.
[6] Varma DS, Agarwal R, Varma IK. Schok Vibration Digest 1986;56(6):364–9.
[7] Jeong YG, Lee SC, Shin K. J Polym Sci Part B Polym Phys 2008;47(3):276–83.
[8] Jeong YG, Lee KJ, Jo WH, Lee SC. Polymer 2008;49(6):1693–700.
[9] Stewart M, Cox AJ, Naylor DM. Polymer 1993;34(19):4060–7.
[10] Jacques B, Devaux J, Legras R, Nield E. J Polym Sci Part A Polym Chem 1996;34(7):1189–94.
[11] Montaudo G, Puglisi C, Samperi F. Macromolecules 1998;31(3):650–61.
[12] Collins S, Kenwright AM, Pawson C, Peace SK, Richards RW. Macromolecules 2000;33(8):1974–2980.
[13] Jeong YG, Jo WH, Lee SC. Fiber Polym 2004;5(3):245–51.
[14] Bluhm TL, Hamer GK, Marchessault RH, Fyfe CA, Veregin RP. Macromolecules 1986;19(11):2871–6.
[15] Kunioka M, Tamaki A, Doi Y. Macromolecules 1989;22(2):694–7.
[16] Yoo HY, Umemoto S, Kikutani T, Okui N. Polymer 1994;35(1):117–22.
[17] Jeong YG, Jo WH, Lee SC. Macromolecules 2000;33(26):9705–11.
[18] Lee JH, Jeong YG, Lee SC, Min BG, Jo WH. Polymer 2002;43(19):5263–70.
[19] Jeong YG, Jo WH, Lee SC. Macromolecules 2003;36(11):4051–9.
[20] Hoffman JD, Weeks JJ. J Res Natl Bur Stand 1962;66A:13.
[21] Jeong YG, Jo WH, Lee SC. Macromol Res 2004;12(5):459–65.
[22] Flory PJ. J Chem Phys 1947;15:684.
[23] Flory PJ. Trans Faraday Soc 1955;51:848.
[24] Baur VH. Makromol Chem 1966;98:297.
[25] Helfand E, Lauritzen Jr JI. Macromolecules 1973;6(4):631–8.
[26] Sanchez IC, Eby RK. Macromolecules 1975;8(5):638–41.
[27] Wendling J, Suter UW. Macromolecules 1998;31(8):2516–20.
[28] Van Krevelen DW. Properties of polymers. 3rd ed. Amsterdam: Elsevier; 1990.